JOURNAL OF GEOPHYSICAL RESEARCH, VOL. 106, NO. A8, PAGES 15,963–15,971, AUGUST 1, 2001

Scales of heliospheric current sheet coherence between 1 and 5 AU

N. U. Crooker,[1] S. W. Kahler,[2] J. T. Gosling,[3] D. E. Larson,[4] R. P. Lepping,[5]
E. J. Smith,[6] and J. De Keyser[7]

Abstract. The structure of the heliospheric current sheet (HCS) at Ulysses and at Wind is compared during the period of near-radial alignment in 1998. Electron heat flux and magnetic field data are used to determine true magnetic field polarity. During the solar rotation period surrounding alignment there was considerable disagreement between the HCS crossings at Wind and those predicted from the corresponding source surface map, both in number and in location, consistent with the disordered, temporally varying solar wind at this ascending phase of the solar cycle. Despite this complexity the four crossings closest to the time of radial alignment at Wind were successfully identified in Ulysses data with use of a one-dimensional hydrodynamic code. Further, minimum variance analysis for the first two crossings, which were separated by only 16 hours at Wind, indicated coherent propagation of a large-scale warp in the HCS. Analysis of the local structure of the HCS on the four crossings, however, revealed a high level of variability both from case to case and from one spacecraft to the other. For example, the third crossing at Wind was a single-sheet crossing adjacent to structures with fields folded back on themselves and a brief period of counterstreaming electrons implying a transient structure. At Ulysses multiple sheets were encountered. At the fourth crossing Wind passed through a counterstreaming event with a flux rope signature containing a south pointing axis, while Ulysses passed through a flux tube with little field rotation and northward pointing field. The results are consistent with the view that the heliospheric current sheet is coherent as a global structure but highly variable in local structure over angular distances of a few degrees.

1. Introduction

Few opportunities arise to study the coherence of the heliospheric current sheet (HCS) between nearly radially aligned spacecraft. One of these occurred during the declining phase of solar cycle 20, in 1974, when Pioneers 10 and 11, located at ~4 AU and ~6 AU, respectively, were nearly aligned for about seven solar rotations, one of which included alignment with the Earth-orbiting IMP spacecraft, as well. The period was dominated by two giant recurrent streams, which created a series of corotating interaction regions containing the HCS [*Thomas and Smith*, 1981]. Because of the high degree of order in the heliosphere at that time, characteristic of the declining phase, matching HCS crossings between spacecraft was a relatively straightforward task. *Siscoe and Intriligator* [1993, 1994] analyzed a number of these matched crossings by comparing observed transit times to calculated transit times based on the average speed of the HCS at the two spacecraft. They found a surprising degree of variability but argued that corrections for the dynamic effects of stream interactions and deviations from Parker spiral HCS orientations could account for most of the variability. The structure of the HCS at each crossing was not addressed in these studies.

A second opportunity to study the HCS with nearly aligned spacecraft occurred during the ascending phase of solar cycle 23, in 1998, when Ulysses, at aphelion, slowly moved southward across the ecliptic plane at 5.4 AU while Wind, tied to Earth's ecliptic orbit around the Sun, crossed Ulysses' longitude. The heliosphere was much less ordered during this period. For the four-month period surrounding closest alignment on February 26, *De Keyser et al.* [2000] show complex sector structure at Wind which is difficult to match by eye with the sector structure at Ulysses. De Keyser et al. were able to match many pairs of individual HCS crossings, however, with application of a one-dimensional hydrodynamic code, supporting the claim by *Siscoe and Intriligator* [1993, 1994] that stream interactions can account for much of the discrepancy produced by constant speed mapping. De Keyser et al. analyzed the structure of the HCS at three of the sharpest crossings observed at Ulysses. The study presented here builds on their work by analyzing and intercomparing four different HCS crossings at Ulysses and Wind, the four which occurred closest to radial alignment.

2. Predicted and Observed Sector Structure at 1 AU

Plate 1 places the sector boundary crossings of interest into the context of the global heliospheric pattern during the peri-

[1]Center for Space Physics, Boston University, Boston, Massachusetts.
[2]Air Force Research Laboratory, Space Vehicles Directorate, Hanscom Air Force Base, Massachusetts.
[3]Los Alamos National Laboratory, Los Alamos, New Mexico.
[4]Space Sciences Laboratory, University of California, Berkeley.
[5]Laboratory for Extraterrestrial Physics, NASA Goddard Space Flight Center, Greenbelt, Maryland.
[6]Jet Propulsion Laboratory, California Institute of Technology, Pasadena.
[7]Belgian Institute for Space Aeronomy, Brussels.

Paper number 2000JA000109.
0148-0227/00/2000JA000109$09.00

od of near-radial alignment between Ulysses and Wind. The top panel shows a source surface map of coronal fields from the Wilcox Observatory Web site, inverted so that time runs from left to right. It covers the 27 day period February 14 - March 13, 1998, and thus is a composite of the end of Carrington rotation 1932 and most of 1933. The former was included in order to cover all of the sector boundary crossings closest to February 26 at 1 AU, the date of nearest alignment. The map predicts two crossings for this solar rotation period, indicated by the thin lines extending downward from the intersection of the neutral line with Earth's path across the map, where the neutral line is the boundary between fields pointing toward and away from the Sun.

The schematic panel below the map shows how the predicted crossings would appear on a pitch angle spectrogram for electrons in the heat flux energy range of ~100-400 eV, and the third panel shows the observed pitch angle spectrogram for 230 eV electrons measured at Wind. The spectrograms are lagged by 4 days to account for the solar wind transit time to Earth. Since heat flux always flows away from the Sun along the magnetic field, it indicates toward polarity when it flows antiparallel to the field and away polarity when it flows parallel to the field. Thus maximum flux (red) at the top of the spectrogram, where the pitch angle is 180°, indicates a toward sector and, at the bottom, where the pitch angle is 0°, indicates an away sector.

Comparison between the predicted and observed spectrograms reveals considerable disagreement, much more so than is usual for source surface map comparisons with in situ data at 1 AU [e.g., *Behannon et al.*, 1989; *Burton et al.*, 1994]. The second predicted sector boundary, on February 27, lines up with an observed crossing, but the first does not, and at least five crossings are observed where none are predicted. The disagreement may be owing to temporal changes in coronal fields in the ascending phase of the solar cycle, evidenced in the major pattern changes between successive source surface maps surrounding this period (not shown) and in the disordered nature of the solar wind. Many nonrecurrent, small-scale streams appeared at Wind during this period and, for the most part, dissipated by the time they reached Ulysses [*Gosling et al.*, 1999; *Crooker et al.*, 1999]. This pattern contrasts greatly with the 1974 pattern observed by the Pioneer and IMP spacecraft during the descending phase, as described above, when the highly ordered, two-stream pattern maintained itself over the same radial distances.

The most outstanding deviation of the observed from the predicted pattern in Plate 1, the March 4-10 away sector in the middle of what should have been a toward sector, was initiated by a coronal mass ejection (CME). The leading edge of a magnetic cloud on March 4, identified by Lepping et al. (Profile of a generic magnetic cloud at 1 AU for the quiet solar phase: WIND observations, submitted to the *Journal of Geophysical Research*, 2000) (hereinafter referred to as Lepping et al., submitted manuscript, 2000), brought the field polarity change from toward to away. The field rotation in the cloud is apparent in the plot of magnetic azimuth angle ϕ_B in the bottom panel, and some evidence of intermittent counterstreaming electrons (simultaneously parallel and antiparallel to the field) signifying closed CME fields can be found in the spectrogram throughout the sector. Further analysis of ACE and Ulysses data for this event is given by *Skoug et al.* [2000]. Since the CME most likely arose from the vicinity of the neutral line just north of Earth's path across the map in this interval, it is surprising that its polarity did not blend in with the sector structure, as it does for most interplanetary CMEs (ICMEs) [*Zhao and Hoeksema*, 1996; *Kahler et al.*, 1999]. The configuration might be related to the polarity of newly emerging flux on the Sun, which, during the ascending phase of the solar cycle, is opposite to that of the overlying flux from the weakening solar dipolar field of the previous cycle [cf. *Wang et al.*, 2000].

Of primary concern in the present study are the sector boundary crossings labeled 1-4 under the spectrogram in Plate 1. These occurred closest to the February 26 alignment date, marked with a solid triangle. Crossings 1, 2, and 4 appear clearly in the magnetic azimuth plot, as well, where the average Parker spiral angles are marked with dashed lines. Crossing 3 is also apparent there but is much clearer in the spectrogram. The contrast is examined at higher resolution in section 4. In section 3 we map these crossings to Ulysses, and the resulting matching pairs are analyzed in detail in sections 4-6.

3. Mapping to 5.4 AU

To map crossings 1-4 from Wind to Ulysses, we use the results of *De Keyser et al.* [2000], who mapped all of the polarity reversals in Wind magnetic field data during a four-month period surrounding alignment using a one-dimensional (or spherically symmetric) gas-dynamic code. The mapping was carried out to 5 AU, at the longitude of Wind, which we take to be Earth's longitude. To derive predicted crossing times, we extended the mapping to 5.4 AU using the simpler constant-speed (ballistic) method and added times appropriate to corotation over the short longitudinal distance between Earth and Ulysses. The resulting predicted crossing times are indicated in the top panel of Figure 1. Remarkably, they line up well enough with the observed crossings, apparent in the magnetic azimuth variations in the second panel, to allow an unambiguous association. We note that the less accurate method of ballistic mapping through the full radial distance between Wind and Ulysses also gives unambiguous associations in these cases, although the predicted crossing times by this method are further from the observed times for three of the four crossings. The ability to map crossings from Wind to Ulysses successfully confirms the conclusions of the earlier studies that the heliospheric current sheet is a coherent global structure over large radial distances. In contrast, sections 4-6 show a lack of coherence in local HCS structure between the two spacecraft.

4. Crossing 3

We begin our comparison of local HCS structure with the most complex crossing, for which the electron heat flux data provide a key analysis tool. Because the electron heat flux is low at 5.4 AU, details of sector boundary structure at Ulysses are not easy to read from a pitch angle spectrogram. Instead, Figure 1 provides a plot of the quantity $\mathbf{Q} \cdot \mathbf{B}$, where $\mathbf{B}$ is the magnetic field vector and $\mathbf{Q}$ is the heat flow vector. Normally, $\mathbf{Q}$ is calculated by taking the third moment of the particle distribution. Here, however, $\mathbf{Q}$ was calculated from a bi-Maxwellian fit to the data by subtracting the velocity of the core of the distribution from that of the halo, where the heat flux electrons reside. This procedure yielded a clear $\mathbf{Q} \cdot \mathbf{B}$ signal. Figure 1 shows the results in the bottom panel, plotted so that points at the top indicate toward fields and those at the bottom indicate

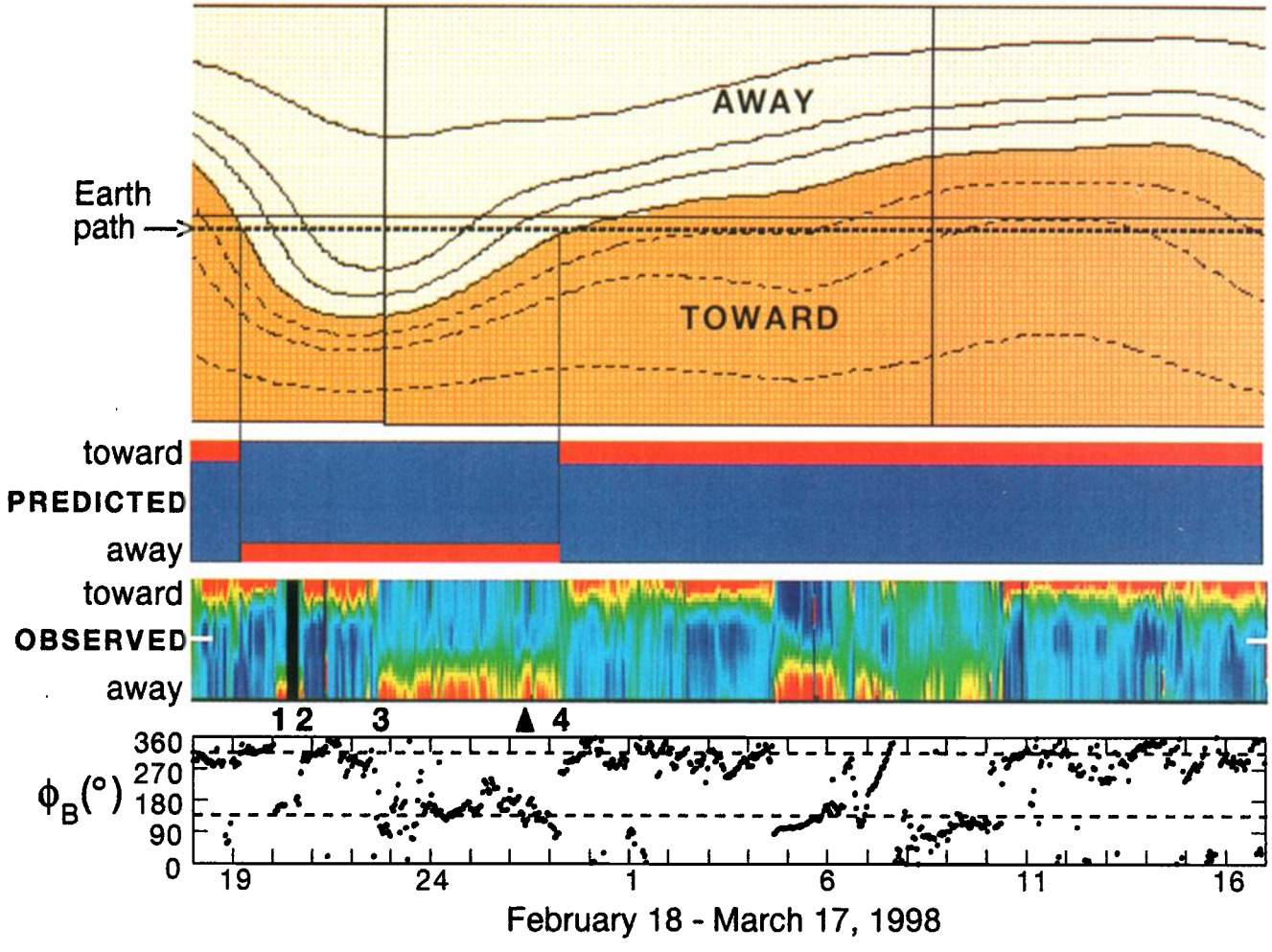

Plate 1. Sector structure predicted from a classic source surface map and compared with observed structure in electron and magnetic field data from Wind at ~1 AU for a period of one solar rotation. The map, in the top panel, is from the Wilcox Observatory Web site. It is pieced together from maps for Carrington rotations 1932 and 1933, inverted so that time increases from left to right, and displaced by 4 days with respect to the data to acount for solar wind propagation to 1 AU. The two vertical lines extending from top to bottom mark the beginning and middle of CR 1933. The two thinner vertical lines extending downward from the intersection of the neutral line with Earth's path mark predicted sector boundary crossings. The second and third panels are predicted and observed heat flux electron pitch angle distributions. Maximum flux is indicated by the red end of the spectrum. It appears at the top of a spectrogram if it is antiparallel to the magnetic field and at the bottom if parallel, corresponding to toward and away sectors, as marked. The numbers beneath identify the four crossings closest to the time of near-radial alignment of Wind with Ulysses. This time is marked with a solid triangle. The bottom panel shows time variations of hourly averages of the magnetic field azimuth angle in GSE coordinates. Points near the top (bottom) dashed line indicate fields pointing toward (away from) the Sun along the Parker spiral.

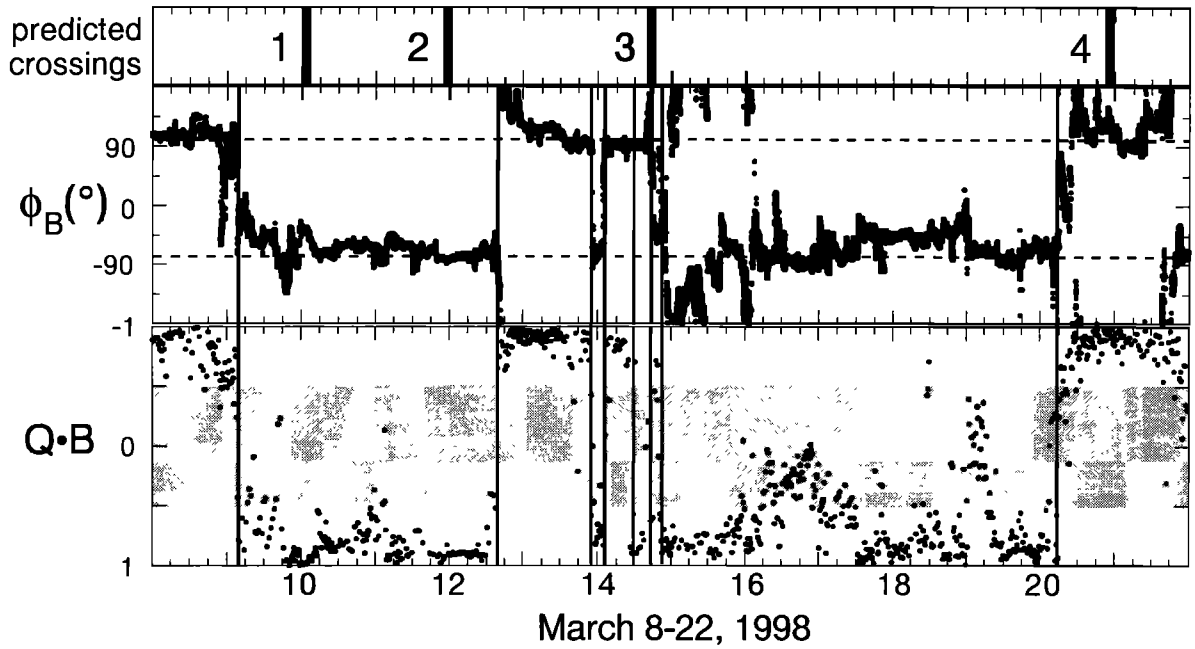

Figure 1. Predicted and observed sector structure at 5.4 AU. The top panel shows the predicted times of sector boundary crossings at Ulysses obtained by mapping the crossings from Plate 1 with use of a hydrodynamic code. The second panel shows time variations of the magnetic field azimuth angle at Ulysses in RTN coordinates, with dashed lines at the average Parker spiral angles, and the third panel shows the dot product of the electron heat flux vector **Q** and the magnetic field direction **B**. Both plots indicate toward and away polarity in the same sense as the plots in Plate 1. The vertical lines in the lower two panels mark the true sector boundary crossings determined from the **Q** • **B** plot.

away fields, consistent with spectrogram presentation. Points falling in the shaded region are inconclusive and should be ignored, since ideally, **Q** • **B** should equal 1 or -1. In spite of these points the sector structure is clear. Vertical lines mark the true polarity reversals, where **Q** • **B** changes sign.

Here we focus on crossing 3, which appears to consist of five polarity reversals at Ulysses, as marked, although only a few points indicate the last pair. The magnetic azimuth angle in the middle panel reflects the first two reversals, remains steady through the third, and reverses in an opposite sense across the fourth. At the fifth the field begins a complicated excursion through more than 360° which takes more than a day to complete, while its true polarity holds steady. The disjunction between true polarity and magnetic field direction in the interval between the third and fifth reversals indicates adjacent flux tubes of opposite polarity folded or coiled back on themselves. Contrary to some expectations [e.g., *Villante et al.*, 1979; *Behannon et al.*, 1981; *Suess et al.*, 1995; *Bavassano et al.*, 1997; *De Keyser et al.*, 2000], the data do not match the alternating global-local current sheet pattern required for waves in the HCS [*Crooker et al.*, 1996a], which does not accommodate true polarity reversals with no coincident magnetic field reversals, as in the case of the third reversal.

The pattern at Wind for crossing 3 was also complicated but in a different way. Plate 2 shows the high-resolution electron and field data for the day surrounding the crossing. Although the magnetic azimuth angle in the bottom panel is highly variable, the pitch angle spectrogram shows a single polarity reversal, just prior to 1500 UT, in contrast to the multiple reversals at Ulysses. The reversal was preceded and succeeded by periods when the magnetic azimuth angle pointed in directions opposite to the true toward and away field polarities, respectively, implying fields turned back on themselves, as marked, but there were no true polarity reversals in these intervals. (Note that owing to the scale break at 360°, not all excursions between top and bottom reflect large angular changes.) Earlier still were two periods of counterstreaming or bidirectional electrons (BDEs) indicating closed, transient structures, although the first of these is questionable owing to the large imbalance between the flux antiparallel to the field compared to that parallel to the field.

Whether the difference in pattern at Wind and Ulysses is spatial or temporal or both (most likely) cannot be determined. If spatial, then a parameter of interest is the scale over which the pattern varied in longitude and latitude compared to radial distance. If the former is much larger than the latter, for example, then different structure at the two crossings is not unexpected. At Ulysses the 4.7° angular separation of the spacecraft (2.7° in latitude and 3.8° in longitude) corresponds to 0.44 AU, compared to the 0.20 AU scale of the radial span of multiple reversals. Thus the distance over which the pattern varied along the spherical surface perpendicular to the radial direction was only about twice as large its radial span. This ratio is small, especially in view of the fact that convected structures in a spherically expanding medium must kinematically elongate in the direction orthogonal to their radial depth merely to maintain their angular span [cf. *Crooker et al.*, 1996b]. At Wind the scale size ratio was similar. The angular separation of the spacecraft corresponds to 0.08 AU, compared to the 0.05 AU scale of the radial span of the HCS crossing including the surrounding fields turned back on themselves. This result is somewhat surprising, since in an ideal wind, with no dynamic interactions, the radial spans at the two spacecraft should be the same, while spacecraft separation dis-

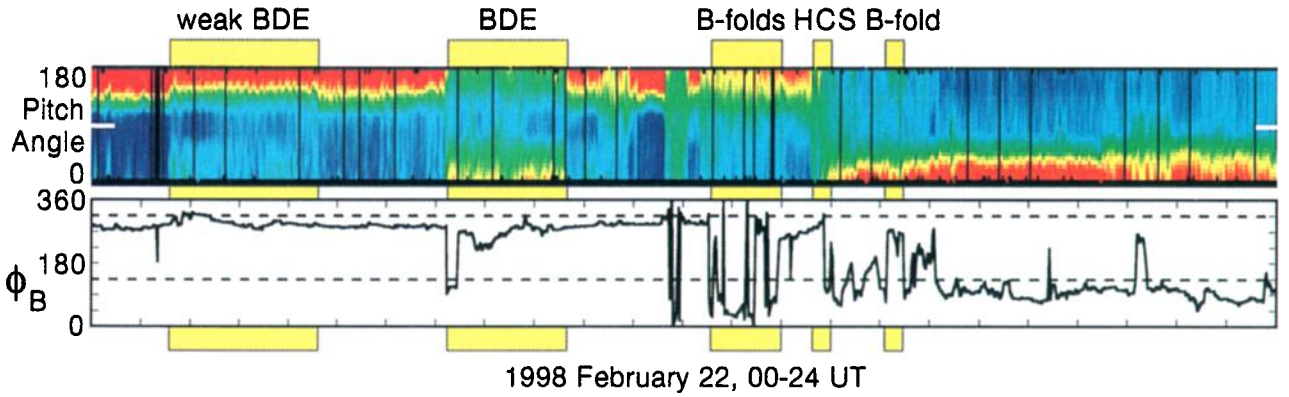

Plate 2. High-time-resolution plot of the Wind electron and field data from Plate 1 for crossing 3. Yellow bars highlight the HCS crossing and intervals of bidirectional electrons (BDEs) and fields turned back on themselves (*B* folds).

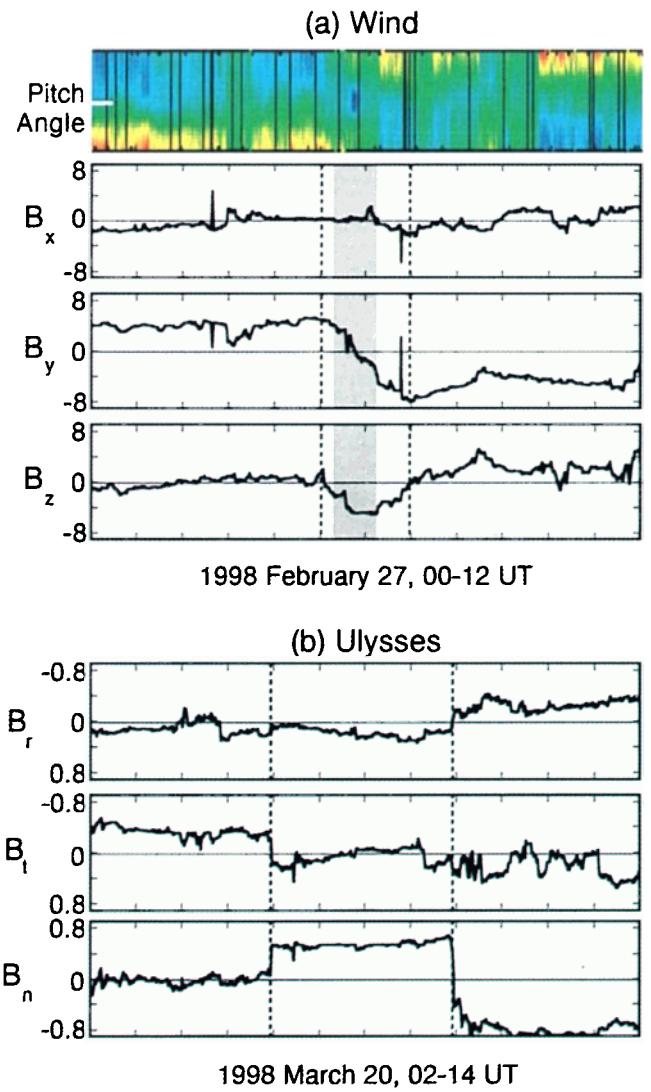

Plate 3. Magnetic field components at crossing 4, in (a) GSE coordinates at Wind and (b) RTN coordinates at Ulysses, with B_r and B_t inverted for direct comparison. Shading in Plate 3a indicates bidirectional electrons, as seen in the pitch angle spectrogram in the top panel. Vertical dashed lines outline flux rope structure in Plate 3a and flux tube structure in Plate 3b.

tance increases linearly with radial distance. This result, coupled with the proximity of BDEs to the HCS at Wind and model predictions of gross distortions of transient structures as they propagate outward [e.g., *Odstrcil and Pizzo*, 1999], suggests that temporal variations contributed substantially to the difference between HCS structure at Wind and that at Ulysses.

5. Crossing 4

The sector boundary crossing closest to the time of nearest spacecraft alignment occurred in a single polarity reversal at Wind and Ulysses, apparent in the electron data on February 27 in Plate 1 and on March 20 in Figure 1, respectively. On the other hand, the polarity reversals were carried by clearly different magnetic structures at the two spacecraft. The GSE field components plotted in Plate 3a show that the reversal at Wind was carried by a relatively smooth flux-rope-like structure, outlined with vertical dashed lines. The negligible B_x, the smooth change in B_y from positive to negative, and the negative dip in B_z are signatures similar to those found on a much larger scale in magnetic clouds (e.g., *Lepping et al.*, submitted manuscipt, 2000). They indicate a rope with a southward directed axis and right-hand chirality. Minimum variance through the structure gives a normal primarily in the x direction, as expected from these variations. The top panel in Plate 3a is a high-resolution pitch angle spectrogram. It shows about an hour-long interval of counterstreaming electrons at the polarity reversal. Mapped down as shading in the field plots, the interval covers a portion of the flux rope structure, indicating that it is partially magnetically closed, as commonly found in magnetic clouds [*Shodhan et al.*, 2000]. The small size of this structure, however, combined with no distinguishing temperature signature, places it in the category of ropes identified by *Moldwin et al.* [2000], who argue that their origin is magnetic reconnection across the HCS.

We note that field rotations across the HCS are common signatures and that flux rope interpretations of data from single-spacecraft measurements are not unique (see discussion by *Crooker et al.* [1993] and references therein). For example, *Behannon et al.* [1981] interpret rotations as signatures of a uniform, distributed current sheet. A distributed current that gives a rotational signature, however, must correspond to some kind of transient outflow or, if steady state, some kind of skewing of coronal fields in the streamer belt [cf. *Eselevich and Filippov*, 1988]. In view of the variability of local HCS structure we choose the flux rope interpretation as the more likely option.

Plate 3b gives magnetic field data for crossing 4 at Ulysses, where the field components are plotted in RTN coordinates. Since, in the ecliptic plane, RTN and GSE components are roughly the same except for opposite signs of the first two, the B_r and B_t scales are inverted to facilitate comparison with Plate 3a. The magnetic polarity reversal was carried by a discrete magnetic structure which appears to be a flux tube with field directed primarily northward ($+B_n$). Its boundaries are marked with dashed lines, where the reversal in the ecliptic plane takes place primarily by a change in the sign of B_t at the left line and a change in the sign of B_r at the right. The electron heat flux data indicate that the true polarity change occurred at the left (leading) edge so that the structure itself had its roots in the Sun's southern heliomagnetic hemisphere. The weak B_r and B_t components in the structure display minor rotation, indicating a minor degree of helicity (toroidal fields dominate poloidal fields), similar to flux tubes found in a case study of another HCS crossing at Ulysses [*Crooker et al.*, 1996b]. Although the chirality is the same as that of the flux rope at Wind and the degree of helicity of a convecting flux rope is expected to decrease with distance from the Sun [*Cargill et al.*, 2000], the predominant northward field in the flux tube at Ulysses is opposite to the southward field in the rope at Wind. Thus the structures cannot be the same.

The different structures at Wind and Ulysses at crossing 4 imply a spatial variation on the scale of their 2.7° angular separation (2.5° in latitude and 1.0° in longitude) at that time, which corresponds to 0.05 AU at Wind and 0.25 AU at Ulysses. As for crossing 3, the radial span of the HCS structure is shorter at Wind than at Ulysses, 0.014 AU and 0.04 AU, respectively. These numbers indicate that the spacecraft separation was 4-6 times larger than the radial scale of the HCS structures. Apparently this distance is large enough to preclude intersection of the same structure, in spite of the mitigating effects of kinematic elongation.

6. Crossings 1 and 2

Whereas crossings 3 and 4 were considerably different from each other at the two spacecraft, crossings 1 and 2 show some degree of similarity. Figure 2, in the same format as Plate 3, gives magnetic field component plots for Wind and Ulysses, in this case for both crossings 1 and 2, marked with vertical lines. The two crossings occurred on the same day at Wind, February 20, and on March 9 and March 12 at Ulysses. The crossing times were taken from the electron heat flux data. They were single crossings within the resolution of the data except for crossing 2 at Wind, where a ~5 min excursion back into the away sector occurred ~15 min after the primary crossing. In general, the crossings from the heat flux data line up well with the polarity reversals in the magnetic field.

Crossings 1 and 2 may have marked the boundaries of an ICME. At Wind, crossing 1 coincided with the onset of an approximately hour-long interval of counterstreaming electrons, as marked by the shaded region in Figure 2a, consistent with closed ICME fields there. Additional intervals of counterstreaming occurred sporadically throughout the region between the two crossings (outside the data gap). These are not marked because they may have been caused by backstreaming electrons from Earth's bow shock, to which Wind was magnetically connected, instead of by closed ICME fields. At Ulysses an interval of counterstreaming was found prior to crossing 1, at ~1600-2200 UT on March 8, as marked. Between the crossings, from ~1200 UT on March 9 to ~1200 UT on March 12, a steady but highly unbalanced interval of counterstreaming occurred, with very weak flux antiparallel to the field, again making the identification of closed ICME fields uncertain. On the other hand, combined with the relatively smooth variations in B_t and B_n for most of the interval between the crossings, apparent in the middle and bottom panels of Figure 2b, the signatures at Ulysses, like those at Wind, suggest ICME passage, although other plasma signatures are lacking.

Focusing on the structure at crossing 1 in Figure 2, one can see that the magnetic polarity reversal takes place in steps leading up to the marked crossing, so that the field reversal is essentially triple. That is, the B_x and B_y components at Wind and the B_r and B_t components at Ulysses change sign 3 times. The signature is clearer in the Wind data, where it lasts for about a half hour, or 0.005 AU. At Ulysses the signature ap-

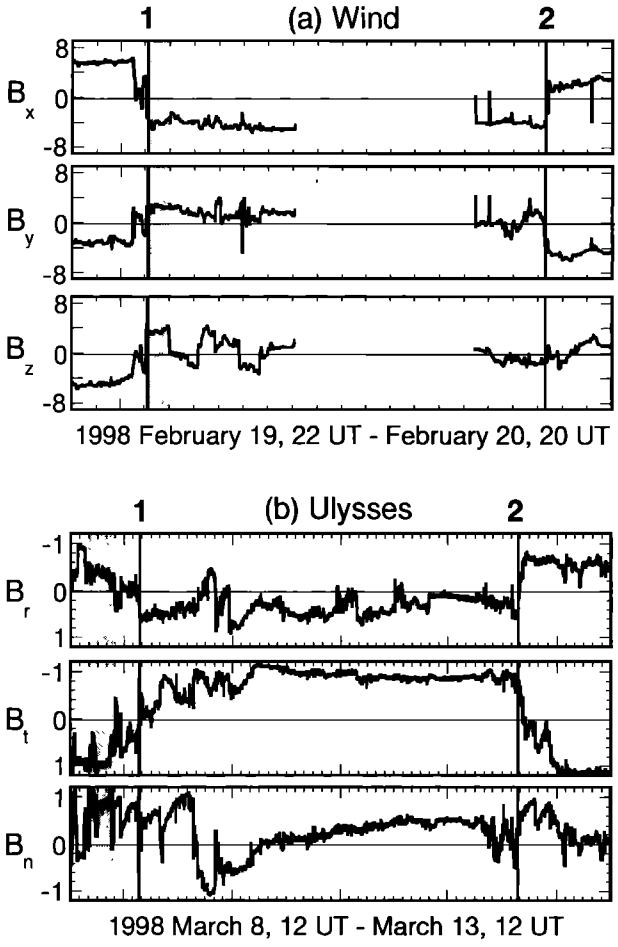

Figure 2. Magnetic field components at crossings 1 and 2, in (a) GSE coordinates at Wind and (b) RTN coordinates at Ulysses, with B_r and B_t inverted for direct comparison, in the same format as Plate 3. Solid vertical lines mark true sector boundary crossings determined from the high-resolution electron data from Wind (not shown) and the Ulysses **Q** • **B** plot in Figure 1.

pears immediately after the shaded BDE interval and lasts longer, as in crossings 3 and 4, ~6 hours, or 0.06 AU. Since the angular separation of the spacecraft was 6.9° (3.0° in latitude and 6.3° in longitude), corresponding to 0.12 AU at Wind and 0.67 AU at Ulysses, the separation was 24 and 11 times larger than the radial widths, respectively. Because these ratios are considerably larger than for crossings 3 and 4, where no coherence of local structure was evident, the suggested coherence in this case seems serendipitous.

Whether the crossing 1 structure was a true triple reversal or created by fields turned back on themselves cannot be determined at Wind because the electron distribution became isotropic there [cf. *Pilipp et al.*, 1987], obscuring any polarity information. The Ulysses heat flux data in Figure 1, however, show no interval of opposite polarity during the first two magnetic reversals and thus do indicate fields turned back on themselves at that location. Minimum variance analysis across the triple magnetic reversal yields a hodogram with rotational oscillations suggesting passage through a wavy HCS, similar to what *De Keyser et al.* [2000] found for the January 7-8 sector boundary crossing, although on a larger scale. In this case, however, the heat flux data rule out that interpretation. The HCS was crossed only once at Ulysses, and local current sheets created the magnetic reversals prior to that crossing.

The orientation of the HCS at crossing 1 was determined by minimum variance analysis across the triple magnetic reversal, treating it as a complex or "thick" crossing, following *Klein and Burlaga* [1980]. The angles between the normals to the surfaces at the two spacecraft differed by ~55°. Most of this difference was in the sense of steepening of the surface between Wind and Ulysses. That is, the surface normals move closer to the ecliptic plane with distance from the Sun, as might be expected from both kinematic (spherical expansion) and dynamic effects [e.g., *Thomas and Smith*, 1981; *De Keyser et al.*, 2000].

Crossing 2 had no particularly distinctive features, although the local structure was somewhat different at the two spacecraft. As mentioned above, the electron data from Wind show a 5 min return to the away sector after the primary crossing. A comparable excursion is not apparent in the Ulysses data, but this may reflect the poorer temporal resolution there. The magnetic reversal at Ulysses was carried by what appears to be about a 4-hour-long discrete magnetic structure, the initial boundary of which forms the HCS identified in the heat flux data, similar to crossing 4. The field clearly rotates across the structure, suggestive of a flux rope, although many small-scale fluctuations are superposed on the rotation. In contrast to the different local structures at the two spacecraft for crossing 2, minimum variance analysis across them indicates similar surface orientations, with an angle of ~30° between the surface normals. As in the case of crossing 1, the difference was primarily in the sense of steepening of the surface between Wind and Ulysses.

The deduced orientations of the HCS surfaces at crossings 1 and 2, considered as a pair, provide a coherent view consistent with radial passage of a large-scale warp in the HCS. Figure 3 illustrates the geometry projected onto a meridional plane. The heavy lines indicate the HCS tilts in that plane for crossings 1 and 2 at each spacecraft, as labeled. The tilts at Ulysses are steeper, as expected, and the sense of the tilts at both spacecraft indicates passage through the trough of a large-scale warp propagating out from the Sun [cf. *De Keyser et al.*, 2000, Figure 2]. A trough configuration is consistent with passage through an intrusion of the away sector from above and thus consistent with the global polarity pattern of the source surface map in Plate 1. Like the later, 6 day intrusion of the away sector beginning on March 4 in Plate 1, the intrusion between crossings 1 and 2 may have been caused by an ICME, as discussed above.

7. Discussion and Conclusions

The four crossings of the heliospheric current sheet by nearly radially aligned spacecraft at 1 AU and 5.4 AU analyzed in this study show a wide variety of local structure but coherence on a global scale. Global coherence was reflected both in the ability to match crossings at the two locations, in spite of the high variability in the solar wind at the time, and in the ability to fit the deduced HCS inclinations for the two most closely spaced crossings to passage through the trough of a global wave. At the local level, however, none of the crossings at either location had structure consistent with a wavy current sheet. The local structure ranged in pattern from a series of true multiple crossings to single crossings accompanied by fields turned back on themselves to crossings carried by discrete flux

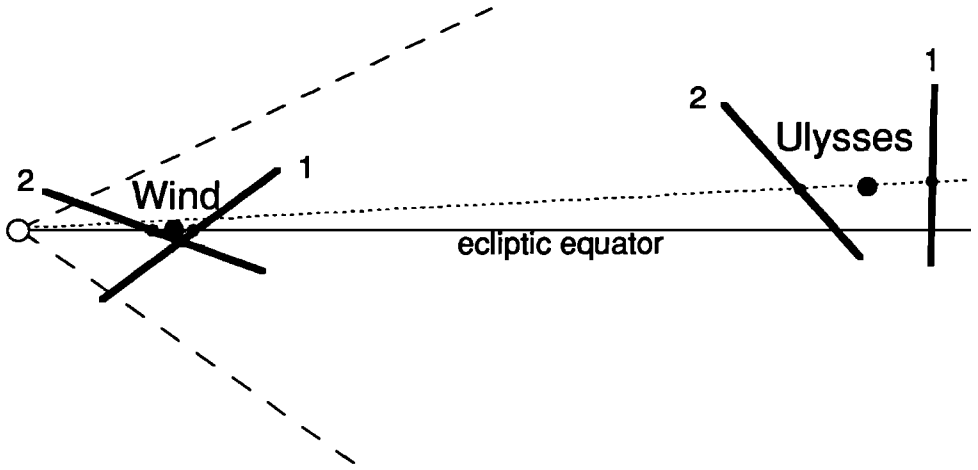

Figure 3. HCS surface orientations at Wind and Ulysses in the meridional plane of crossings 1 and 2, indicated by heavy lines tangent to the surface at the measuring points. The dashed lines encompass the latitudinal span of HCS excursions for the full solar rotation, for comparison. The excursion implied by the surface orientations is shallower but steepens between Wind and Ulysses.

ropes or tubes. Only one of the four crossings showed similar local structure at the two locations.

As deduced from earlier studies (see review by *Crooker* [1999]), Figure 4 schematically illustrates the kind of local structure that is consistent with the observations. It shows a magnified view of a cross section of the HCS covering ~2° of latitude and ~3° of longitude. It has the form of a network of flux tubes and ropes of mixed magnetic polarities. Some of the tubes may turn back on themselves, in which case their true polarities would oppose the illustrated magnetic polarities. The small arrows in the regions bounding the flux tubes indicate current flow. Together these constitute the total current in the HCS, flowing predominantly from left to right, consistent with the global polarity pattern. Although the network in Figure 4 pinches down to a single curent sheet at either end, in reality the longitudinal scale size is probably unlimited. That is, the network may extend, with variable thickness, along the entire HCS surface. Also not illustrated is the idea that the flux tube cross sections are likely to be distended or flattened along the surface, owing to spherical expansion and, sometimes, to compression [*Crooker et al.*, 1996b].

The lines labeled a-d in Figure 4 are sample trajectories across the structure for a variety of HCS orientations. Line a represents the ideal crossing through a single current sheet with no structure on either side. It fits none of the crossings analyzed in this study. Lines b and c represent crossings with multiple magnetic polarity reversals, like crossings 1 and 3. They can be either true multiple polarity reversals, like crossing 3 at Ulysses, or one true reversal mixed with local reversals, like crossing 3 at Wind. While the signature along line b could, in isolation, be interpreted as passage through parallel multiple sheets extending from multiple helmet structure on the Sun [*Crooker et al.*, 1993] and the signature along line c could be interpreted as passage through a wavy current sheet,

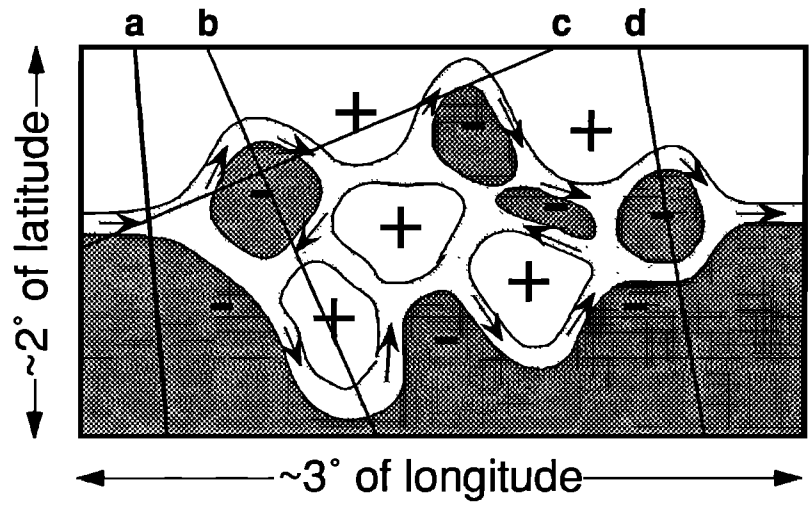

Figure 4. Schematic drawing of a cross section of the HCS illustrating local structure. Flux tubes and ropes of opposite polarity meet and intertwine. Current in the HCS flows primarily around the boundaries of these tubes, as indicated by the arrows. The lines marked a-d illustrate hypothetical trajectories through the structure, which will produce a variety of signatures.

the structure as a whole is neither of those. Line d represents passage through a single flux tube or rope, like crossing 4. It illustrates a subtle distinction between true and magnetic polarity reversals: The polarity of the tube/rope is the same as that of the southern heliomagnetic hemisphere, so that the true polarity change is across its northern boundary; however, current flows within the tube, as well, so that the magnetic polarity reversal is distributed across the tube. If the tube were a rope on a much larger scale, constituting an ICME, a horizontal line through its crest would represent an ICME-caused intrusion of opposite polarity, similar (although opposite in sense) to the March 4 event and, possibly, to the pair of crossings 1 and 2. Overall, the Figure 4 view of the HCS synthesizes a number of competing ideas about its structure.

In conclusion, this study has demonstrated that in the spirit of the pioneering work of *Kahler and Lin* [1994, 1995], electron data provide a valuable tool for analyzing sector boundaries. With data from nearly radially aligned spacecraft during a period of complicated sector structure unmatched by source surface map predictions, we have shown that the heliospheric current sheet is coherent on a global scale but highly variable in its local structure. The results are consistent with the HCS as the meeting plane of flux tubes/ropes of opposite polarity which, at times, can form a jumbled network covering several degrees of longitude and latitude, most likely as a result of both small-scale transient outflows and turbulence.

Acknowledgments. This research was an outgrowth of collaborative efforts at the 1998 Ulysses Aphelion Workshop in Oxnard, California. It was supported by NASA under grants NAG5-6658 and NAG5-7049. Work at Los Alamos was performed under the auspices of the U.S. Department of Energy, also with support from NASA.

Janet G. Luhmann thanks Mark B. Moldwin and Steven T. Suess for their assistance in evaluating this paper.

References

Bavassano, B., R. Woo, and R. Bruno, Heliospheric plasma sheet and coronal streamers, *Geophys. Res. Lett., 24*, 1655-1658, 1997.

Behannon, K. W., F. M. Neubauer, and H. Barnstorf, Fine-scale characteristics of interplanetary sector boundaries, *J. Geophys. Res., 86*, 3273-3287, 1981.

Behannon, K. W., L. F. Burlaga, J. T. Hoeksema, and L. W. Klein, Spatial variation and evolution of heliospheric sector structure, *J. Geophys. Res., 94*, 1245-1260, 1989.

Burton, M. E., N. U. Crooker, G. L. Siscoe, and E. J. Smith, A test of source-surface model predictions of heliospheric current sheet inclination, *J. Geophys. Res., 99*, 1-9, 1994.

Cargill, P. J., J. Schmidt, D. S. Spicer, and S. T. Zalesak, Magnetic structure of overexpanding coronal mass ejections: Numerical models, *J. Geophys. Res., 105*, 7509-7519, 2000.

Crooker, N. U., Heliospheric current sheet structure, in *Solar Wind Nine*, edited by S. Habbal et al., *AIP Conf. Proc., 471*, 93-98, 1999.

Crooker, N. U., G. L. Siscoe, S. Shodhan, D. F. Webb, J. T. Gosling, and E. J. Smith, Multiple heliospheric current sheets and coronal streamer belt dynamics, *J. Geophys. Res., 98*, 9371-9381, 1993.

Crooker, N. U., M. E. Burton, G. L. Siscoe, S. W. Kahler, J. T. Gosling, and E. J. Smith, Solar wind streamer belt structure, *J. Geophys. Res., 101*, 24,331-24,341, 1996a. (Correction, *J. Geophys. Res., 102*, 4741. 1997.)

Crooker, N. U., M. E. Burton, E. J. Smith, J. L. Phillips, and A. Balogh, Heliospheric plasma sheets as small-scale transients, *J. Geophys. Res., 101*, 2467-2474, 1996b.

Crooker, N. U., G. L. Siscoe, J. T. Gosling, J. T. Steinberg, A. J. Lazarus, and D. S. Intriligator, Entropy increase in slow solar wind from damping of large-scale structures between 1 AU and 5 AU (abstract), *Eos Trans. AGU, 80*(17), Spring Meet. Suppl., S269, 1999.

De Keyser, J., M. Roth, R. Forsyth, and D. Reisenfeld, Ulyssses observations of sector boundaries at aphelion, *J. Geophys. Res., 105*, 15,689-15,698, 2000.

Eselevich, V. G., and M. A. Filippov, An investigation of the heliospheric current sheet (HCS) structure, *Planet. Space Sci., 36*, 105-115, 1988.

Gosling, J. T., D. J. McComas, D. B. Reisenfeld, J. T. Steinberg, and A. J. Lazarus, A comparison of predicted and observed solar wind structure at Ulysses using Wind observations and a simple numerical code (abstract), *Eos Trans. AGU, 80*(17), Spring Meet. Suppl., S265, 1999.

Kahler, S., and R. P. Lin, The determination of interplanetary magnetic field polarities around sector boundaries using $E>2$ keV electrons, *Geophys. Res. Lett., 21*, 1575-1578, 1994.

Kahler, S., and R. P. Lin, An examination of directional discontinuities and magnetic polarity changes around interplanetary sector boundaries using $E>2$ keV electrons, *Sol. Phys., 161*, 183-195, 1995.

Kahler, S. W., N. U. Crooker, and J. T. Gosling, The polarities and locations of interplanetary coronal mass ejections in large interplanetary magnetic sectors, *J. Geophys. Res., 104*, 9919-9924, 1999.

Klein, L., and L. F. Burlaga, Interplanetary sector boundaries 1971-1973, *J. Geophys. Res., 85*, 2269-2276, 1980.

Moldwin, M. B., S. Ford, R. Lepping, J. Slavin, and A. Szabo, Small-scale magnetic flux ropes in the solar wind, *Geophys. Res. Lett., 27*, 57-60, 2000.

Odstrcil, D., and V. J. Pizzo, Three-dimensional propagation of coronal mass ejections (CMEs) in a structured solar wind flow, 1. CME launched within the streamer belt, *J. Geophys. Res., 104*, 483-492, 1999.

Pilipp, W. G., H. Miggenrieder, K.-H. Mülhäuser, H. Rosenbauer, R. Schwenn, and F. M. Neubauer, Variations of electron distribution functions in the solar wind, *J. Geophys. Res., 92*, 1103-1118, 1987.

Shodhan, S., N. U. Crooker, S. W. Kahler, R. J. Fitzenreiter, D. E. Larson, R. P. Lepping, G. L. Siscoe, and J. T. Gosling, Counterstreaming electrons in magnetic clouds, *J. Geophys. Res.*, in press, 2000.

Siscoe, G., and D. Intriligator, Three views of two giant streams: Aligned observations at 1 AU, 4.6 AU, and 5.9 AU, *Geophys. Res. Lett., 20*, 2267-2270, 1993.

Siscoe, G., and D. Intriligator, Macroscale coherence of the heliospheric current sheet: Pioneers 10 and 11 comparisons, *Geophys. Res. Lett., 21*, 2075-2078, 1994.

Skoug, R. M., W. C. Feldman, J. T. Gosling, D. J. McComas, D. B. Reisenfeld, C. W. Smith, R. P. Lepping, and A. Balogh, Radial variation of solar wind electrons inside a magnetic cloud observed at 1 and 5 AU, *J. Geophys. Res.*, in press, 2000.

Suess, S. T., D. J. McComas, S. J. Barne, and B. E. Goldstein, Solar wind eddies and the heliospheric current sheet, *J. Geophys. Res., 100*, 12,261-12,273, 1995.

Thomas, B. T., and E. J. Smith, The structure and dynamics of the heliospheric current sheet, *J. Geophys. Res., 86*, 11,105-11,110, 1981.

Villante, U., R. Bruno, F. Mariani, L. F. Burlaga, and N. F. Ness, The shape and location of the sector boundary surface in the inner solar system, *J. Geophys. Res., 84*, 6641-6652, 1979.

Wang, Y.-M., N. R. Sheeley Jr., and N. B. Rich, Evolution of coronal streamer structure during the rising phase of solar cycle 23, *Geophys. Res. Lett., 27*, 149-152, 2000.

Zhao, X.-P., and J. T. Hoeksema, Effect of coronal mass ejections on the structure of the heliospheric current sheet, *J. Geophys. Res., 101*, 4825-4834, 1996.

N. U. Crooker, Center for Space Physics, Boston University, 725 Commonwealth Avenue, Boston, MA 02215. (crooker@bu.edu)

J. De Keyser, Belgian Institute for Space Aeronomy, Ringlaan 3, B-1180 Brussels, Belgium. (johan.dekeyser@oma.be)

J. T. Gosling, Los Alamos National Laboratory, MS D466, Los Alamos, NM 87545. (jgosling@lanl.gov)

S. W. Kahler, Air Force Research Laboratory, Space Vehicles Directorate, 29 Randolph Road, Hanscom Air Force Base, MA 01731-3010. (Stephen.Kahler@hanscom.af.mil)

D. E. Larson, Space Sciences Laboratory, University of California, Berkeley, CA 94720. (davin@ssl.berkeley.edu)

R. P. Lepping, Laboratory for Extraterrestrial Physics, NASA Goddard Space Flight Center, Code 696.0, Greenbelt, MD 20771. (rpl@leprpl1.gsfc.nasa.gov)

E. J. Smith, Jet Propulsion Laboratory, MS 169-506, 4800 Oak Grove Drive, Pasadena, CA 91109. (esmith@jplsp.jpl.nasa.gov)

(Received May 1, 2000; revised July 5, 2000;
accepted July 5, 2000.)